Position and Velocity Cursor Mappings Contribute to Distinct Muscle Forces in Simulated Isometric and Movement Reaching

Margaret P. Chapman, Michele F. Rotella, and Allison M. Okamura, *Fellow IEEE*

***Abstract*—Contributions of muscle forces in isometric and normal (movement) reaching have not been thoroughly compared. In this study, we ask if position-based and velocity-based cursor mappings during planar isometric reaching produce muscle forces that are similar to those exerted during unassisted movement. Healthy subjects pushed against a static manipulandum handle to direct a cursor toward a target using either a position or velocity mapping. Applied force and cursor path data were used to create dynamic musculoskeletal simulations (using the OpenSim platform) of targeted isometric and movement reaches. Isometric muscle forces in both position and velocity mappings were found to be distinct from the corresponding forces in movement simulations. These results motivate future research on the design of a physiology-based isometric mapping that incorporates arm dynamics and inertia. A mapping that produces comparable muscular activity in isometric and movement reaching may support the development of improved isometric and robotic rehabilitation strategies for patients with upper limb movement deficits.**

I. Introduction

Task-oriented repetitive movement therapy is commonly used to improve upper limb motor function in patients with stroke and other neurological disorders [1]. Robot-assisted rehabilitation offers several benefits over conventional techniques, including reduced physical labor of therapists, novel modes of exercise, and built-in mechanisms to quantify performance [2]. Isometric reaching, in which the user applies force/torque onto a static sensor in order to control a virtual cursor, offers a potential rehabilitation method for patients with upper limb movement deficits. A previous study showed that isometric torque training of the elbow and shoulder reduced abnormal muscle coactivation in patients with moderate to severe stroke [3]. Isometric training is safe for impaired individuals [4, 5] and can be tailored to meet evolving patient-specific needs throughout treatment [4].

The relationship between muscle forces in isometric and movement reaching should be understood in order to enable the design of novel, isometric-based rehabilitation strategies that effectively target subject-specific deficits. While neural activity [6, 7] and muscular electrical signals (i.e. EMG) [8] during various isometric tasks have been studied, the contributions of muscles in force production for isometric and movement reaching have not been compared. Few, if any, feasible methods exist to measure detailed muscle forces experimentally, but simulation provides a viable alternative to obtain reasonable estimates. We use OpenSim, a modeling and simulation tool that enables dynamic simulation of human motion and estimation of internal loading of the musculoskeletal system [9]. Such tools allow researchers to obtain critical information about muscular activity that could be extremely difficult or impossible to obtain otherwise.

This work was supported in part by a National Science Foundation Graduate Research Fellowship.

M. P. Chapman, M. F. Rotella, and A. M. Okamura are with the Department of Mechanical Engineering, Stanford University, Stanford, CA 94305. (Email: aokamura@stanford.edu)

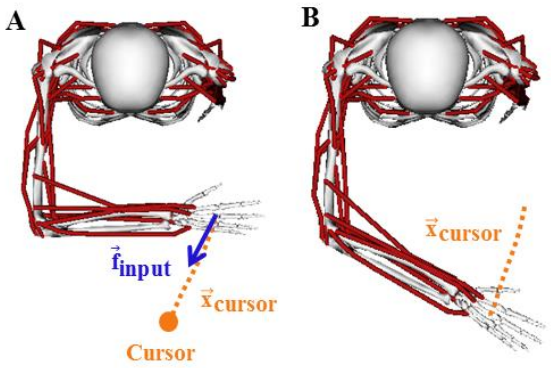

Fig. 1. Musculoskeletal model simulations of planar isometric and movement reaches. A. In the isometric reach, a stationary arm exerts force to control a cursor. B. In the movement reach, the arm moves in free-space along the cursor path.

In this paper, we utilize recorded human isometric reaching data in combination with a newly released upper limb OpenSim model, based on [10] but with reduced degrees of freedom, to estimate muscle forces during planar isometric and movement reaching (Fig. 1). Data of applied force at the hand and cursor position were recorded from healthy human subjects and used to generate muscle force simulations. We aimed to compare muscle forces during isometric and movement reaching using position-based and velocity-based cursor mappings, and identify which type of mapping, if any, produces comparable forces in the isometric and movement cases. We present a repeatable process for examining muscle forces in reaching, and provide a foundation for future analysis that encompasses multiple reaching directions across the workspace. The results of this work contribute to knowledge of how isometric training may translate to upper limb motor function.

II. Background

A. Isometric Force Control

Isometric force control, or targeted force exertion by a static limb, has been studied primarily in the upper extremity to investigate basic attributes of the neuromuscular system.

Since isometric reaching is similar to movement, yet not subject to inertial or viscoelastic resistance [8], it is useful for examining the fundamentals of human motor control and developing new theoretical frameworks. Ultimately, a deeper understanding of neuromuscular control may lead to more effective treatments for people with motor deficits.

Toward this end, prior work in isometric control has explored synergistic muscle activation and motion planning. EMG recordings of isometric elbow torques revealed that most muscle synergies of the elbow are task-dependent [11, 12]. This suggests that elbow muscles within the same functional group (e.g. elbow extensors) may be similarly activated when performing an isometric reaching task. Neural activity was also examined during isometric reaching in the transverse plane to investigate the role of the motor cortex in motion planning [7]. The results indicated that the motor cortex helps transform motor output from extrinsic to intrinsic coordinates in isometric upper limb tasks. Muscle forces, the focus of our study, deserve careful investigation since they influence intrinsic coordinates (i.e. joint positions) directly and generate motion, often with error in impaired individuals.

B. Comparison between Isometric and Movement Reaching

Some studies have investigated how physiological behavior compares during isometric and movement tasks, with mixed results. EMG activity of primate arm muscles was analyzed during isometric and movement reaching in eight radially-symmetric planar directions; EMG profiles were found to exhibit "ramp-like" and "triphasic" trends in the isometric and movement conditions, respectively [6]. Such differences in muscle activation suggest that differences in muscle force will also exist between movement and isometric reaching.

While [6] shows dissimilarity, there is some evidence that parallels exist in *learning* of isometric and movement tasks. Adaptation to a kinematic perturbation (i.e. visual cursor rotation) was investigated during planar isometric and movement reaching by healthy subjects; the rate of adaptation, which signifies motor learning, was found to be comparable in the isometric and movement conditions [13]. Moreover, similar limitations in shoulder/elbow torque production were discovered in a study that examined isometric and movement tasks performed by hemiparetic stroke patients; during both tasks, production of elbow extension torques was reduced during exertion of shoulder abduction torques [4]. Evidence of similarities between isometric and movement reaching supports investigations of isometric training for future applications in rehabilitation.

To our knowledge, no prior work has investigated the comparison of muscle forces during isometric and movement reaching, most likely due to the difficulty of measuring muscle forces experimentally. While studies of pure muscle forces are needed to understand muscular physiological behavior [12], investigations in the isometric control literature are limited to EMG recordings. Surface EMG recordings cannot easily isolate individual muscles, and intramuscular EMG requires an invasive procedure. The work we present here uses simulation to fill this gap in knowledge.

C. OpenSim Musculoskeletal Simulation

OpenSim is an open-source software tool that allows the creation of dynamic simulations of subject-specific musculoskeletal models and the estimation of quantities, such as internal muscle loads, that are difficult to measure experimentally [9]. This tool has helped researchers study motor pathologies [14], coordinated lower extremity motion [15], and simulated surgery [16]. Additionally, OpenSim has been used for isometric force/torque analysis. A clinically-relevant model was developed with OpenSim software for estimating muscle contributions to ankle joint moment during isometric and movement tasks [17]. Also, torque measured from an experiment was compared to torque simulated from an OpenSim model for isometric ankle plantar flexion to investigate model accuracy; correction parameters were found to reduce error [18]. In this paper, we simulated planar isometric and movement reaches on a new upper body model currently under review. The musculoskeletal properties and geometry of this model are from [10], but with reduced degrees of freedom, and the muscle control algorithm is adopted from [19]. OpenSim's static optimization tool was used to solve for the unknown muscle forces in our simulations. The details of our experimental and simulation protocols are described in the following section.

III. METHODS

In this study, the goal was to compare muscle forces of healthy subjects in isometric and movement reaching using two cursor mappings. Subjects performed a center-out isometric reach to a single target (Fig. 2). Input force and cursor path data were used to simulate the isometric reach and a movement reach along the cursor path in OpenSim software. OpenSim's static optimization toolbox was implemented to compute shoulder and elbow muscle forces.

A. Upper Limb Isometric Reaching Experiment

1) Experimental Setup: An isometric reach was performed by two right-handed, healthy subjects of similar dimensions and weight (Position Map Subject: height = 1.676 m, weight = 61.23 kg, upper arm length = 0.305 m; Velocity Map Subject: height = 1.727 m, weight = 66.22 kg, upper arm length = 0.305 m). Force measured at the hand was used to control a cursor, with the goal of acquiring a target positioned 45° from the +*x*-axis (Fig. 2). To complete this task, subjects interacted with a two-degree-of-freedom planar manipulandum, which is described in [13]. Throughout our data collection, the links of the device were mechanically locked in place, and the subjects grasped the handle. The handle had an embedded 6-axis force/torque sensor (ATI Mini-45), which measured force applied by the subject in the planar *x*-*y* directions. Forces were sampled at 1 kHz and filtered using a second-order, discrete Butterworth filter with 6 Hz cut-off frequency. Sensor resolution was 0.125 N, and forces below 0.2 N in magnitude were discarded. Subjects were seated in a stationary chair with shoulder restraints to limit excessive movement of the upper torso. The forearm was physically supported against gravity, and subjects wore noise-isolating headphones for comfort. A mirror-projection system was used for viewing the target and cursor from a computer monitor, such that the hand was spatially aligned with the cursor. The arm was occluded at all times.

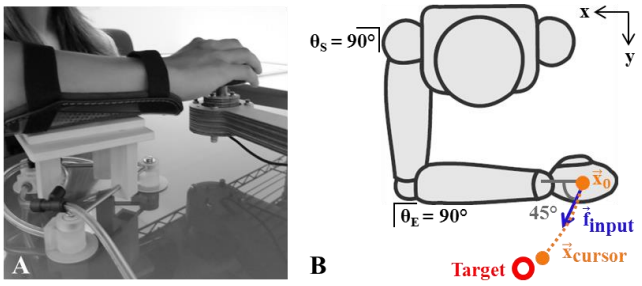

Fig. 2. Upper limb planar isometric reach. A. Experimental platform consisting of manipulandum, visual display, and body restraint/support mechanisms. B. A subject exerts force, $\vec{f}_{input}$, in the *x*-*y* plane to direct a cursor toward a stationary target positioned 45° from the +*x*-axis in the positive sense, at a distance of 10 cm from the initial cursor position, $\vec{x}_0$. The arm was positioned with the shoulder angle, θ_S, and elbow angle, θ_E, equal to approximately 90°.

2) Force Calibration and Cursor Mappings: The cursor was controlled using a position or velocity mapping from input force to cursor movement. These mappings were calibrated for each subject to accommodate individual strength. During calibration, subjects were asked to apply force (minimum of 20 N) that they would feel comfortable maintaining for 10 s in 4 separate directions ($\pm x$, $\pm y$), following the display of wedge-shaped targets. Subjects applied forces in each direction for 3 s, and the smallest peak force across all directions was selected as the calibration force, f_{cal}. In the position mapping, cursor position, $\vec{x}_{cursor} = (x, y)^T$, was found by scaling the input force by the position gain, k_p:

$$\vec{x}_{cursor} = k_p * \vec{f}_{input} \quad (1)$$

$$k_p = c_p / f_{cal}. \quad (2)$$

Likewise, in the velocity mapping, the input force was directly mapped to the velocity of the cursor via a gain, k_v:

$$\dot{\vec{x}}_{cursor} = k_v * \vec{f}_{input} \quad (3)$$

$$k_v = c_v / f_{cal}. \quad (4)$$

The control constants, selected empirically and modified slightly from those used in [13] to improve cursor responsiveness, were c_p = 0.24 m and c_v = 1.5 m/s, respectively.

3) Experiment Protocol: Throughout the experiment, the subject's arm was positioned with the shoulder angle, θ_S, and elbow angle, θ_E, equal to 90° (Fig. 2). The arm was kept in plane with the shoulder as much as possible, though all arm positions were approximate and varied slightly given differences in subject size. Each subject pushed against the static manipulandum handle to direct a cursor toward a circular target, located 10 cm from the initial cursor position directly below the hand. Subjects were instructed to make quick, accurate movements of the cursor for 40 trials. Cursor velocity was found using numerical differentiation and filtered with a second-order discrete-time filter (8 Hz cut-off frequency). Subjects received feedback between trials on the maximum cursor speed using a graphical speedometer display; desirable speed range was 0.4 to 0.6 m/s.

4) Data Analysis and Selection: Cursor position and force data were recorded at 500 Hz. To identify the start of cursor movement, components of position data were filtered using a second-order, low-pass Butterworth filter (6 Hz cut-off frequency), applied in forward and reverse order. For each trial, movement onset was determined by searching backward from the peak speed to find where the speed dropped 5% below the maximum. A position-mapped trial and a velocity-mapped trial with approximately straight cursor paths and maximum speed within the desired peak speed range were used to create the dynamic musculoskeletal simulations described in the next section.

B. Dynamic Musculoskeletal Simulations in OpenSim

1) Generating the Subject-Specific Model: In order to generate the subject-specific model from [10] using OpenSim's scaling tool, we manually calculated three parameters, including the subject-specific model mass and scale factors for maximum isometric force and segment lengths. The parameters were computed using measurements of subject total mass, m_{subj}, height, h_{subj}, and distance from shoulder to elbow, $d_{SE\ subj}$. The mass of the subject-specific model, $m_{UL\ model*}$, was computed using the following equation:

$$m_{UL\ model*} = m_{subj} * m_{UL\ model} / m_{FB\ model}, \quad (5)$$

where $m_{UL\ model}$ is the mass of the generic upper extremity model, equal to 34.04 kg [10], and $m_{FB\ model}$ is the mass of the full body gait model, equal to 75.16 kg [20]. The maximum isometric muscle forces in the subject-specific model were scaled from the original maximum isometric muscle forces in [10] by $f_{scale\ force}$:

$$f_{scale\ force} = h_{subj} * m_{subj} / (h_{FB\ model} * m_{FB\ model}), \quad (6)$$

where $h_{FB\ model}$ is the height of a 50th percentile male, 1.7 m [10]. Maximum isometric muscle force can also be estimated through ultrasound techniques [21] and dynamometers [22]; calculation by (6) represents a simple alternative when those methods are not practical. Segment lengths of the subject-specific model were scaled uniformly in three-dimensions from the original lengths by $f_{scale\ segment}$:

$$f_{scale\ segment} = d_{SE\ subj} / d_{SE\ model}, \quad (7)$$

where $d_{SE\ model}$ is the distance between the shoulder marker, M_S, and the elbow marker, M_E, on the right arm of the generic upper extremity model, 0.2837 m (Fig. 3).

2) Static Optimization: The static optimization toolbox in OpenSim was used to solve for the unknown muscle forces. Static optimization solves the equations of motion

$$M(\vec{q})\ddot{\vec{q}} + C(\vec{q},\dot{\vec{q}}) + G(\vec{q}) = \vec{\tau}, \quad (8)$$

where N is the number of degrees of freedom, $\vec{q}, \dot{\vec{q}}, \ddot{\vec{q}} \in \mathbb{R}^N$ are vectors of joint position and the derivatives, $M(\vec{q}) \in \mathbb{R}^{N \times N}$ is the mass matrix of the musculoskeletal model, $C(\vec{q},\dot{\vec{q}}) \in \mathbb{R}^N$ is the vector of Coriolis and centrifugal forces, $G(\vec{q}) \in \mathbb{R}^N$ is the vector of gravitational forces, and $\vec{\tau} \in \mathbb{R}^N$ is the vector of unknown joint torques, subject to additional constraints [23]. One constraint is based on muscle force-length-velocity properties, and the second constraint is a minimization function of muscle activation. The force-length-velocity properties are

$$\sum_{m=1}^{n} \{a_m f(F_m^0, l_m, v_m)\}\, r_{m,j} = \tau_j, \quad (9)$$

and the objective function to be minimized is

$$J = \sum_{m=1}^{n} (a_m)^2, \quad (10)$$

where n is the number of muscles in the model, a_m is the activation of muscle m at a discrete time step, F_m^0 is the maximum isometric force of muscle m, l_m is muscle length, v_m is muscle shortening velocity, $f(F_m^0, l_m, v_m)$ is the muscle's force-length-velocity surface, $r_{m,j}$ is the muscle moment arm about the j^{th} joint axis, and τ_j is the joint torque acting about the j^{th} joint axis [24].

3) Isometric Reaching Simulation: The isometric reaching experiment described in Section III.A was simulated on the subject-specific model using OpenSim's static optimization toolbox. External forces against gravity were applied to the center of masses (COM) of the model's right hand, ulna, and radius, equal to each body's respective weight. These forces are necessary because, during the experiment, the subject's hand and forearm rested on the manipulandum handle and arm support, respectively. The subject's input force was applied to the model's hand COM in the simulation. Following our experimental conditions, the shoulder and elbow angles in the simulation (θ_S and θ_E) were set to 90°, and the shoulder abduction angle was also set to 90° to maintain a planar position (Fig. 3). All other joint angles in the model were set to 0°. MATLAB® (The MathWorks, Inc.) was used to generate the files containing external load and kinematic data. The kinematics were filtered at 6 Hz using OpenSim, and static optimization was performed to generate time histories of muscle forces.

4) Movement Reaching Simulation: To study isometric reaching in direct comparison to unassisted movement, we simulated free-space, planar reaching along the cursor path on the subject-specific model. Inverse kinematics were used to compute the shoulder and elbow joint angles needed for the hand to follow the cursor path. Segment lengths were estimated from the subject-specific model using markers placed on the shoulder, elbow, and hand. Joint angles began at 90° to be consistent with the initial conditions of the isometric reach simulation (Fig. 3). MATLAB® was used to generate the kinematic data files. The kinematics were filtered at 6 Hz using OpenSim. No external forces were applied to the upper limb to represent free-space motion. Static optimization was performed to generate time histories of muscle forces during planar reaching.

5) Analysis of Muscle Forces: The isometric and movement reaching simulations previously described were performed for position-based and velocity-based cursor mappings using subject-specific data (one subject for the position mapping, a separate subject for the velocity mapping). We examined shoulder and elbow muscles whose activity ratio, r_a, was greater than 10% in any simulation (i.e. movement or isometric reach, position or velocity mapping). The activity ratio, r_a, is defined for each muscle as:

$$r_a = F_{max}/F_{absolute\ max}, \quad (11)$$

where F_{max} is the maximum force the muscle achieves in simulation, and $F_{absolute\ max}$ is the maximum possible force that the muscle can achieve according to the subject-specific model.

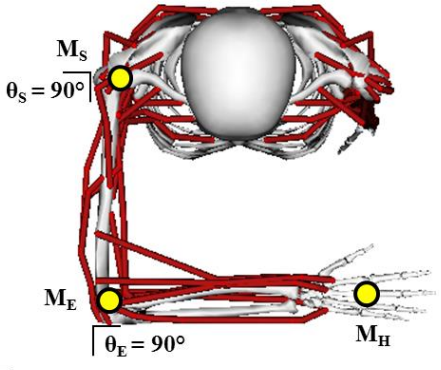

Fig. 3. Position of the active arm throughout the isometric reach simulation, and the initial position during the movement reach simulation. The shoulder angle, θ_S, and elbow angle, θ_E, are equal to 90° to represent experimental conditions. The shoulder marker, M_S, and elbow marker, M_E, were used to compute the distance between the shoulder and elbow joints in the original upper extremity model [10] for segment-length scaling. Distances between M_S and M_E and between M_E and the hand marker, M_H, were used to estimate segment lengths for inverse kinematics.

IV. Results

Fig. 4 shows the input forces and cursor paths for the two subjects during a position-mapped isometric reach (PM) and a velocity-mapped isometric reach (VM). Data is presented from the start of cursor movement to when the target was acquired. In PM, the input force is characterized by an increasing ramp that plateaus. In contrast, the input force in VM is a bell-shaped curve. In both mappings, the corresponding cursor paths are relatively straight, directed toward the target. Slightly different behavior is observed near the path endpoints (i.e. target location). In PM, the cursor oscillates slightly in the vicinity of the target, whereas in VM the cursor overshoots the target and a correction is made.

Fig. 5 shows plots of muscle forces from the simulated isometric and movement reaches for both isometric mappings. The key observations for each mapping are described below.

Position Mapping (Fig. 5A): In PM, the simulated isometric muscle forces are characterized by ramps that increase or decrease to constant values, resembling the shape of the position-mapped input force. While muscle forces resulting from simulated movement have different profiles, several forces show oscillatory behavior (D1, SB, P1), which reflects the small oscillations of the cursor path in Fig. 4. Some muscle force peaks are higher in the isometric reach (D1, SP, IN, SB, TL, TE), whereas others are higher in the movement reach (D2, TM, P1, BL). Specifically, we find that elbow extensors (TL, TE) and most rotator cuff muscles (SP, IN, SB) are more active in the isometric reach, while shoulder abductors (primarily D2 and P1) and the elbow flexor (BL) exert greater forces in the movement reach. Interestingly, the anterior deltoid (D1) has very similar force profiles in the isometric and movement conditions; both plots rise to about 100 N and then remain relatively stable. Typically, we observed greater muscle force ranges in the isometric condition than in the movement condition.

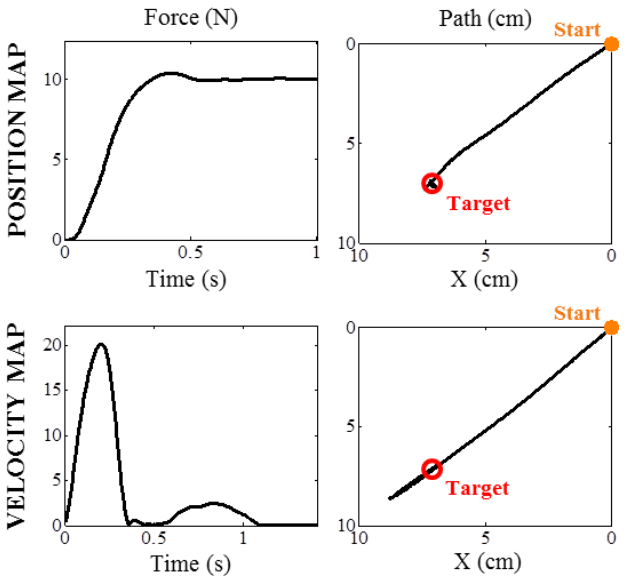

Fig. 4. Input force and cursor path data from the isometric reaching experiment of Section III.A. The position mapping (PM) requires a force ramp that plateaus, whereas the velocity mapping (VM) requires a bell-shaped force that resembles the cursor's speed profile. Both paths are relatively straight initially, and exhibit small oscillations (PM) or overshoot (VM) near the end.

Velocity Mapping (Fig. 5B): In VM, most simulated isometric muscle forces are bell-shaped (D1, D2, SP, IN, SB, TL, TE, BL), similar to the velocity-mapped input force. Most muscle forces resulting from simulated movement tend to reach local extrema and then increase or decrease to constant values (D1, IN, SB, TM, P1, TL, TE, BL). The general shapes of each muscle force in the VM and PM movement simulations are qualitatively similar. Further, overall trends observed in peak muscle forces and ranges in the VM simulations parallel those found in the PM simulations. Specifically, most rotator cuff muscles (SP, IN, SB) and the elbow extensors (TL, TE) exert larger peaks in the isometric condition compared to movement, while most shoulder abductors (D2, P1) and the elbow flexor (BL) follow the opposite trend in both mappings. In both PM and VM, the same groups of muscles demonstrated relatively higher force ranges in the isometric condition (D1, D2, SP, IN, SB, TL, TE) and in the movement condition (TM, P1, BL). One noteworthy exception to PM/VM similarity is the activity of the anterior deltoid (D1). Unlike the position-mapped case, isometric/movement force profiles of D1 in VM do not compare well due to differences in peak force and overall shape. The VM isometric reach requires intense activity of D1 for a short duration, evident in the large peak of 221 N and final value just above 0 N. However, the VM movement reach requires D1 to exert a lower peak force and higher long-term activation.

V. Discussion

We found that simulated isometric and movement reaching result in distinct muscle force profiles using position and velocity cursor mappings. In this section, we discuss the results from each isometric mapping in comparison to movement.

A. Simulated Muscle Forces in Position-Mapped Isometric and Movement Reaching

The overall shapes of the position-mapped muscle forces are derived from experimental force and cursor position inputs. Profiles from the isometric simulation resemble the shape of input force at the hand as input force governs magnitude and timing of muscle activation. However, muscle forces in the movement simulation vary at the end of the reach due to the small oscillations of the cursor path near the target (Fig. 4). The elbow extensors (TL, TE) exert greater forces in the isometric reach because an external load due to the static manipulandum handle opposes elbow straightening; less elbow extensor muscle force is required in the movement reach since the elbow straightens freely without resistance. Conversely, most shoulder abductors play a more dominant role in movement reaching versus isometric, demonstrated by greater peaks of D2 and P1 in movement. This is likely due to the fact that the arm must withstand gravity independently in free space; however, in the isometric reach, external loads that simulate interaction with the physical arm support help maintain the arm's planar position. In addition, high activation of SP, IN, and SB indicates a greater reliance on rotator cuff muscles in the isometric condition compared to movement. This result is somewhat surprising considering that the primary role of these muscles is to maintain shoulder stability and prevent dislocation when the humerus is abducted [25]. We would expect more shoulder stability to be required when the arm is unsupported in movement reaching; however, the isometric reach appears to activate these muscles considerably even when the arm is well supported and stabilized. Further, we found comparable muscular activity of D1 during the isometric and movement conditions, evidence that the position mapping induces similar functional requirements on this muscle. However, as described, this was not a typical finding for most shoulder and elbow muscles.

Clear differences between muscle forces in PM isometric/movement simulations suggest that a pure position mapping may be inadequate for isometric-based rehabilitation. However, the position mapping induces potentially desirable characteristics in muscle activity that should be considered in future mapping designs. Ramp-like isometric muscle forces may be beneficial since they start low and steadily increase, possibly facilitating gradual improvements in arm strength and cursor control. In addition, similar forces of D1 in PM isometric/movement simulations may indicate potential improvement in actions associated with D1, such as humeral abduction, inward rotation, and/or forward reaching [25], with long-term isometric training.

B. Simulated Muscle Forces in VM Isometric/Movement Reaching and their Relation to PM Results

Strong similarities exist between position-mapped and velocity-mapped results. Bell-shaped VM isometric force profiles indicate that VM input force governs overall muscle activation and timing characteristics in the isometric simulation. Likewise, we found an analogous relationship in the position mapping between ramp-like isometric muscle force profiles and input force. Qualitative resemblance between each muscle force profile in VM/PM movement simulations occurs because VM/PM cursor paths are similarly oriented and linear (Fig. 4). Parallel trends in peak

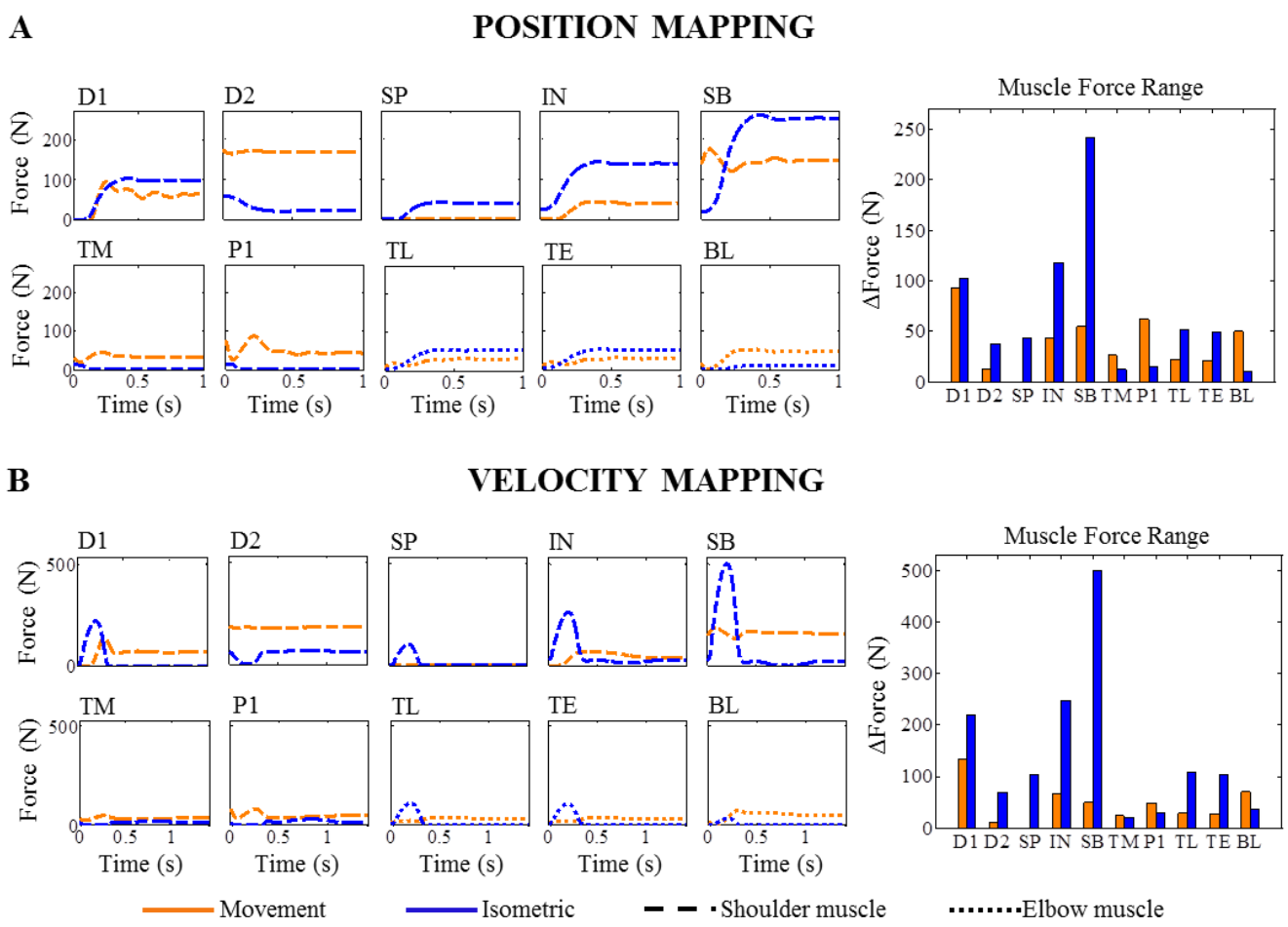

Fig. 5. Force data of the shoulder and elbow muscles in the position-mapped (A) and velocity-mapped (B) simulations. The shoulder muscles are: anterior deltoid (D1), middle deltoid (D2), supraspinatus (SP), infraspinatus (IN), subscapularis (SB), teres minor (TM), and pectoralis major (clavicular head) (P1). The elbow muscles include: lateral triceps (TL), medial triceps (TE), and long biceps (BL). Trends observed in force peaks and ranges comparing the isometric and movement reaches tend to be similar for individual muscles in both mappings. The force profiles of all isometric simulations resemble those of the force input, while the profiles of movement simulations tend to exhibit more complex behavior.

muscle force and range during VM/PM isometric/movement simulations indicate comparable physiological requirements imposed by both mappings. Specifically, the elbow extensors (TL, TE) exert greater peak forces in the isometric reach compared to the movement reach regardless of mapping because the isometric condition imposes external resistance on these muscles while the movement condition permits elbow extension without such resistance. Additionally, the type of mapping does not influence how the arm interacts with gravity, evident by greater peaks of shoulder abductors (primarily D2 and P1) in the movement reach versus the isometric reach in both mappings. Like the pure position mapping, the pure velocity mapping is not necessarily promising for movement rehabilitation due to the clear differences in muscle activity during VM isometric and movement reaching.

Despite strong VM/PM parallels, mapping type does influence the relation between forces of the anterior deltoid (D1) in isometric and movement reaching. Dissimilarity of D1 forces in VM isometric/movement simulations demonstrates that the velocity mapping imposes different functional requirements on D1 during the two reaches. In contrast, we concluded similar functionality of D1 in isometric/movement reaching using the position mapping.

C. Motivation for the Design of a Physiology-Based Mapping

In this study, we found similar relationships in peak muscle force and range between the isometric and movement simulations using the position and velocity mappings. Distinct profiles in position-mapped and velocity-mapped isometric forces were observed, the former ramp-like and the latter bell-shaped. Individual muscles were found to exhibit similar force profiles in the PM and VM movement simulations. Neither the position nor velocity mapping produced comparable muscle forces overall in the isometric and movement reaches. The results of the anterior deltoid (D1) demonstrate that mapping design can influence the relation between functional requirements during isometric and movement reaching.

These preliminary findings motivate several areas of future research. The long-term effects of isometric training, using position-based and velocity-based mappings, on muscle strengthening and motor control should be investigated in healthy and impaired subjects. In addition, a cursor control

mapping that models natural upper limb dynamics during motion should be designed and tested. Different isometric cursor mappings can cause distinct patterns of muscle activity for the same isometric task, as observed in the ramp-like PM isometric muscle forces and the bell-shaped VM isometric muscle forces. A well-constructed mapping could possibly produce comparable muscle forces in isometric and movement simulations. A mapping based on upper extremity physiology, such as acceleration control coupled with arm inertia and damping, may achieve this goal. To date, Berger et al. have implemented an isometric reaching task that attributes mass-spring-damper dynamics to a virtual cursor [26]. In future work, we plan to develop such a mapping, and examine the resulting muscle forces using the protocols presented here. Ultimately, these efforts could lead to the development of novel isometric-based training regimes to facilitate improved motor function in impaired individuals.

ACKNOWLEDGMENTS

The authors thank Dr. Katherine M. Steele for her advice on OpenSim software and for her contributions to the upper extremity model used in this paper, and Margaret Koehler and Mike Rinderknecht for their assistance with experimental setup and data collection.

REFERENCES

[1] L. Oujamaa, I. Relave, J. Froger, D. Mottet, and J. Y. Pelissier. Rehabilitation of arm function after stroke. Literature review. *Annals of Physical and Rehabilitation Medicine*, *52*(3):269-293, 2009.

[2] P. S. Lum, C. G. Burgar, P. C. Shor, M. Majmundar, and M. Van der Loos. Robot-assisted movement training compared with conventional therapy techniques for the rehabilitation of upper-limb motor function after stroke. *Archives of Physical Medicine and Rehabilitation*, *83*(7):952-959, 2002.

[3] M. D. Ellis, B. G. Holubar, A. M. Acosta, R. F. Beer, and J. Dewald. Modifiability of abnormal isometric elbow and shoulder joint torque coupling after stroke. *Muscle & Nerve*, *32*(2):170-178, 2005.

[4] J. P. Dewald, V. Sheshadri, M. L. Dawson, and R. F. Beer. Upper-limb discoordination in hemiparetic stroke: implications for neurorehabilitation. *Topics in Stroke Rehabilitation*, *8*(1):1-12, 2001.

[5] B. H. Dobkin. Strategies for stroke rehabilitation. *The Lancet Neurology*, *3*(9):528-536, 2004.

[6] L. E. Sergio, C. Hamel-Pâquet, and J. F. Kalaska. Motor cortex neural correlates of output kinematics and kinetics during isometric-force and arm-reaching tasks. *Journal of Neurophysiology*, *94*(4):2353-2378, 2005.

[7] L. E. Sergio and J. F. Kalaska. Systematic changes in motor cortex cell activity with arm posture during directional isometric force generation. *Journal of Neurophysiology*, *89*(1):212-228, 2003.

[8] J. J. Pellegrini and M. Flanders. Force path curvature and conserved features of muscle activation. *Experimental Brain Research*, *110*(1):80-90, 1996.

[9] S. L. Delp, F. C. Anderson, A. S. Arnold, P. Loan, A. Habib, C. T. John, E. Guendelman, and D. G. Thelen. OpenSim: open-source software to create and analyze dynamic simulations of movement. *IEEE Transactions on Biomedical Engineering*, *54*(11):1940-1950, 2007.

[10] K. R. Holzbaur, W. M. Murray, and S. L. Delp. A model of the upper extremity for simulating musculoskeletal surgery and analyzing neuromuscular control. *Annals of Biomedical Engineering*, *33*(6):829-840, 2005.

[11] T. S. Buchanan, D. P. Almdale, J. L. Lewis, and W. Z. Rymer. Characteristics of synergic relations during isometric contractions of human elbow muscles. *Journal of Neurophysiology*, *56*(5):1225-1241, 1986.

[12] T. S. Buchanan, G. P. Rovai, and W. Z. Rymer. Strategies for muscle activation during isometric torque generation at the human elbow. *Journal of Neurophysiology*, *62*(6):1201-1212, 1989.

[13] M. F. Rotella, M. Koehler, I. Nisky, A. J. Bastian, and A. M. Okamura. Adaptation to visuomotor rotation in isometric reaching is similar to movement adaptation. In *IEEE International Conference on Rehabilitation Robotics*, pp. 1-6, 2013.

[14] K. M. Steele, M. M. van der Krogt, M. H. Schwartz, and S. L. Delp. How much muscle strength is required to walk in a crouch gait? *Journal of Biomechanics*, *45*(15):2564-2569, 2012.

[15] E. M. Arnold, S. R. Hamner, A. Seth, M. Millard, and S. L. Delp. How muscle fiber lengths and velocities affect muscle force generation as humans walk and run at different speeds. *The Journal of Experimental Biology*, *216*(11):2150-2160, 2013.

[16] A. S. Arnold, M. Q. Liu, M. H. Schwartz, S. Õunpuu, L. S. Dias, and S. L. Delp. Do the hamstrings operate at increased muscle–tendon lengths and velocities after surgical lengthening? *Journal of Biomechanics*, *39*(8):1498-1506, 2006.

[17] P. Gerus, G. Rao, T. S. Buchanan, and E. Berton. A clinically applicable model to estimate the opposing muscle groups contributions to isometric and dynamic tasks. *Annals of Biomedical Engineering*, *38*(7):2406-2417, 2010.

[18] L. L. Menegaldo and L. F. D. Oliveira. Effect of muscle model parameter scaling for isometric plantar flexion torque prediction. *Journal of Biomechanics*, *42*(15):2597-2601, 2009.

[19] D. G. Thelen, F. C. Anderson, and S. L. Delp. Generating dynamic simulations of movement using computed muscle control. *Journal of Biomechanics*, *36*(3):321-328, 2003.

[20] S. L. Delp, J. P. Loan, M. G. Hoy, F. E. Zajac, E. L. Topp, and J. M. Rosen. An interactive graphics-based model of the lower extremity to study orthopaedic surgical procedures. *IEEE Transactions on Biomedical Engineering*, *37*(8):757-767, 1990.

[21] M. Ikai and T. Fukunaga. A study on training effect on strength per unit cross-sectional area of muscle by means of ultrasonic measurement. *Internationale Zeitschrift für Angewandte Physiologie Einschließlich Arbeitsphysiologie*, *28*(3):173-180, 1970.

[22] A. W. Andrews, M. W. Thomas, and R. W. Bohannon. Normative values for isometric muscle force measurements obtained with hand-held dynamometers. *Physical Therapy*, *76*(3):248-259, 1996.

[23] J. Hicks. How inverse dynamics works. *OpenSim 3.0 Documentation*, 2012. Retrieved January 27, 2014, from http://simtk-confluence.stanford.edu:8080/display/OpenSim/How+Inverse+Dynamics+Works.

[24] J. Hicks. How static optimization works. *OpenSim 3.0 Documentation*, 2014. Retrieved January 27, 2014, from http://simtk-confluence.stanford.edu:8080/display/OpenSim/How+Static+Optimization+Works.

[25] N. Hamilton, W. Weimar, and K. Luttgens. *Kinesiology: Scientific Basis of Human Motion*. Boston: McGraw-Hill, 2008.

[26] D. J. Berger, R. Gentner, T. Edmunds, D. K. Pai, and A. d'Avella. Differences in adaptation rates after virtual surgeries provide direct evidence for modularity. *The Journal of Neuroscience*, *33*(30):12384-12394, 2013.